

Differences between the Manganese- and the Iron-Containing Superoxide Dismutases of *Escherichia coli* Detected through Sedimentation Equilibrium, Hydrodynamic, and Spectroscopic Studies[†]

Wayne F. Beyer, Jr., Jacqueline A. Reynolds, and Irwin Fridovich*

Department of Biochemistry, Duke University Medical Center, Durham, North Carolina 27710

Received October 10, 1988; Revised Manuscript Received December 28, 1988

ABSTRACT: The genome of *Escherichia coli* codes for two superoxide dismutases that may contain either iron (FeSOD) or manganese (MnSOD) at the active site. The crystal structures of MnSODs from two bacterial sources (but not *E. coli*) have been completed, and structural comparisons with the crystal structure of the FeSOD from either *E. coli* or *Pseudomonas ovalis* have been made. Despite the low degree (<50%) of sequence homology between the *E. coli* enzymes, the two proteins are suggested to be structurally homologous. Nonetheless, these enzymes exhibit absolute metal cofactor specificity in conferring enzymatic activity to the inactive apoenzyme. This observation is surprising considering the identity of the active site ligands and the similarities in their geometry and surrounding environment. Using analytical ultracentrifugation, we have determined that the solution properties of these two proteins are different. Thus dialysis of FeSOD but not of MnSOD against phosphate buffer in the presence or absence of EDTA caused dissociation of the homodimer. This dissociation appeared to be related to the loss of iron from native FeSOD. Thus, apoFeSOD but not apoMnSOD existed predominantly as a monomer at protein concentrations below 150 $\mu\text{g/mL}$. ApoMnSOD showed no evidence for dissociation under these conditions. Fluorescence data suggest that the tryptophan environments for the two enzymes are also different. The results of these physical measurements lead us to propose that subtle differences, perhaps at the subunit contact faces, exist in the structures of these crystallographically similar proteins.

Escherichia coli can produce two types of superoxide dismutase: one of which contains iron at the catalytic center (FeSOD)¹ while the other contains manganese (MnSOD). The structures, functions, and evolutionary relationship of these enzymes have been reviewed (Bannister et al., 1987; Fridovich, 1986). Currently, X-ray crystal structures have been completed on the FeSODs from *Pseudomonas ovalis* (Ringe et al., 1983) and *E. coli* (Stallings et al., 1983; Carlioz et al., 1988) and on the MnSODs from *Thermus thermophilus* HB8 (Stallings et al., 1985) and *Bacillus stearothermophilus* (Parker & Blake, 1988a). It has been concluded that these enzymes are structural homologues (Stallings et al., 1984; Carlioz et al., 1988).

Yet, the MnSOD and FeSOD of *E. coli* exhibit substantial differences in their solution properties. The subunit mass of FeSOD, calculated from either the deoxynucleotide sequence of its gene (Carlioz et al., 1988) or the results of amino acid sequence analysis (Schinina et al., 1987), is 21 100 Da, whereas the corresponding mass for a subunit of MnSOD is 22 900 Da (Takeda & Avila, 1986; Steinman, 1978). The FeSOD subunit is 192 amino acid residues in length, while the MnSOD subunit contains 205 residues. The FeSOD of *E. coli* has an isoelectric point of 4.5, contains 2.0 ± 0.1 atoms of Fe/molecule, can be inactivated by H_2O_2 , and has a specific activity of 5000 units/mg (Beyer & Fridovich, 1987). The corresponding MnSOD has an isoelectric point of 7.0, contains 1.3 ± 0.5 atoms of manganese per molecule, is not inactivated by H_2O_2 , and exhibits a specific activity of 4500 units/mg (Beyer

& Fridovich, 1986). In addition, these enzymes exhibit substantial differences in their sensitivity to azide inhibition, which allows them to be distinguished in crude cell lysates (Misra & Fridovich, 1978).

The metal binding sites of FeSOD and MnSOD are reportedly identical chemically, containing three histidine residues and one aspartate residue in a trigonal-bipyramidal (Stallings et al., 1985; Carlioz et al., 1988) or strongly distorted tetrahedral arrangement (Parker & Blake, 1988a,b). A water molecule may occupy the fifth coordination position in either the *E. coli* FeSOD or *T. thermophilus* MnSOD (Stallings et al., 1985; Carlioz et al., 1988) but is absent in the *B. stearothermophilus* MnSOD (Parker & Blake, 1988a). Both metals are present in the trivalent oxidation state in the resting enzymes. Nevertheless, the *E. coli* enzymes exhibit absolute metal cofactor specificity. Thus the apoprotein of MnSOD can be restored to full activity by manganese salts but not at all by iron salts, while the apoprotein prepared from FeSOD exhibits the opposite specificity, being reactivated by iron but not by manganese salts. Both proteins are capable of binding stoichiometric amounts of either iron or manganese, and metal competition studies suggest that binding occurs at the active site (Ose & Fridovich, 1976; Beyer & Fridovich, 1987). This specificity is puzzling in light of structural similarities and the virtually identical ligand geometries. Several anaerobes have been reported to contain SODs, which are active with either manganese or iron at the active site; but these have not yet been structurally characterized and compared with the *E. coli*

[†] This work was supported by research grants from the National Science Foundation, the Council for Tobacco Research-U.S.A., Inc., and the National Institutes of Health.

* Author to whom correspondence should be addressed.

¹ Abbreviations: SOD, superoxide dismutase; MnSOD, manganese-containing superoxide dismutase; FeSOD, iron-containing superoxide dismutase; SDS, sodium dodecyl sulfate; DTT, dithiothreitol; R_s , Stokes radius; CD, circular dichroism; KPi , potassium phosphate.

enzymes (Martin et al., 1986; Pennington & Gregory, 1986; Meier et al., 1982).

We have undertaken hydrodynamic, sedimentation equilibrium, and spectroscopic studies of the FeSOD and MnSOD of *E. coli*, primarily to expose differences in their solution properties.

MATERIALS AND METHODS

FeSOD and MnSOD were isolated from *E. coli* B (ATCC 29682) as previously described (Beyer & Fridovich, 1987; Keele et al., 1970). These enzymes were homogeneous as judged by electrophoresis in polyacrylamide gels, both in the native (Davis, 1964) and in the SDS-denatured (Laemmli, 1970) states. The specific activities of the pure enzymes, measured in terms of the xanthine oxidase/cytochrome *c* assay (McCord & Fridovich, 1969), were 5000 units/mg for FeSOD and 4500 units/mg for MnSOD. Protein concentrations were determined spectrophotometrically with $A_{280\text{nm}}^{1\%} = 25.4 \text{ cm}^{-1}$ for FeSOD (Beyer & Fridovich, 1987) and $A_{280\text{nm}}^{1\%} = 18.9 \text{ cm}^{-1}$ for MnSOD (Beyer and Fridovich, unpublished results). The method of Murphy and Kies (1960) was used to estimate the concentration of apoFeSOD. This was done in the absence of DTT, which interferes with this method.

Iron was removed from FeSOD in the presence of 5.0 mM DTT, as described by Yamakura and Suzuki (1976). During this procedure the dialysis buffers were scrubbed continuously with N_2 . The apoFeSOD so produced contained less than 0.02 mol of Fe/42 200 g of protein and exhibited less than 0.5% of the native activity. Iron was determined by atomic absorption spectrophotometry as previously described (Beyer & Fridovich, 1987). ApoFeSOD was stored at 4 °C in 50 mM potassium phosphate at pH 7.8, which had been treated with Chelex-100 to remove adventitious metals and which contained 5 mM DTT. Reconstitution was achieved by anaerobic incubation of 150 $\mu\text{g/mL}$ apoFeSOD, containing 6.7 μM active sites, with 67 μM ferrous ammonium sulfate in 50 mM potassium phosphate + 2.5 mM DTT for 12 h at 25 °C followed by dialysis against several changes of anaerobic 50 mM KPi + 0.1 M EDTA. The reconstituted enzyme exhibited an activity of 4700 units/mg.

Hydrodynamic and sedimentation equilibrium properties were examined with a Beckman Model E analytical ultracentrifuge equipped with ultraviolet optics. Sample volumes were $\sim 100 \mu\text{L}$, at initial $A_{280\text{nm}} = 0.2\text{--}0.4$, for equilibrium sedimentation and were $\sim 300 \mu\text{L}$ at $A_{280\text{nm}} = 1.5$ for sedimentation velocity. Sedimentation coefficients were measured as a function of concentration and extrapolated to zero protein concentration.

Circular dichroism was investigated with a Jobin-Yvon Dichrograph Mark V, which was interfaced with an Apple IIe computer. Samples were maintained at 20 °C, and data were taken at 0.1-nm intervals. The spectra presented here represent averages of three to five scans. The instrument was calibrated with *d*-10-camphorsulfonic acid, $[\theta]_{192.5\text{nm}}/[\theta]_{290.5\text{nm}} = -2.00$ (Yang et al., 1986).

Fluorescence emission was examined with an Aminco-Bowman spectrofluorometer. Samples were maintained at 25 °C and were excited at 280 nm. Sample volumes were 1.0 mL, and protein concentration was less than 100 $\mu\text{g/mL}$ to minimize self-masking.

Gel filtration chromatography was done with an LKB "GTI" biocompatible HPLC system. The column was a TSK SW-3000, and the elutrient was 200 mM potassium phosphate at pH 7.0, used at a flow rate of 0.25 mL/min. $A_{280\text{nm}}$ was recorded. Injection volumes were 10–25 μL . The column was calibrated with proteins of known properties, purchased from

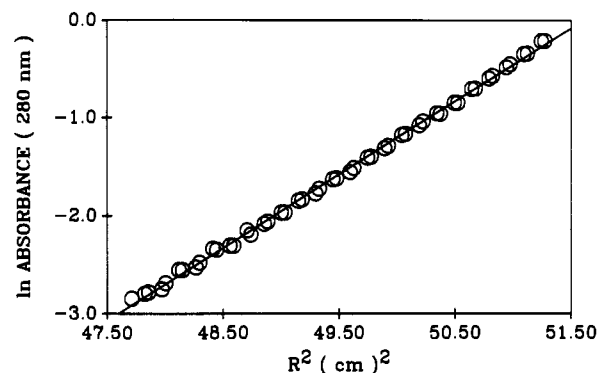


FIGURE 1: Sedimentation equilibrium of MnSOD. The purified enzyme was dialyzed against 50 mM KPi (pH 7.8) buffer containing 0.1 mM EDTA. The protein was brought to equilibrium at 18 000 rpm. The ultracentrifuge was equipped with a photoelectric scanner. The $\ln \text{OD}_{280\text{nm}}$ is plotted as a function of the square of the distance from the center of rotation (R^2).

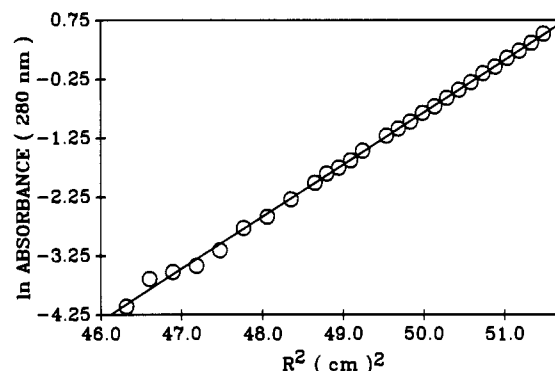


FIGURE 2: Sedimentation equilibrium of MnSOD. The same conditions as in Figure 1 except that the enzyme was dialyzed against 200 mM KPi (pH 7.0) prior to analysis.

Table I: Sedimentation Equilibrium of MnSOD in Phosphate Buffer at 18 000 rpm

	potassium phosphate ^a (50 mM)	potassium phosphate ^b (200 mM)
temp (°C)	15.00	17.34
ρ (g/mL)	1.006	1.018
slope	$0.8851 \pm 8.03 \times 10^{-3}$	$0.7924 \pm 3.74 \times 10^{-3}$
$M(1 - \phi'\rho)$	1.194×10^4	1.077×10^4
M^c	$45\,825 \pm 500$	$43\,027 \pm 250$

^aSupplemented with 0.1 mM EDTA, pH 7.8. ^bpH 7.0. ^cUsing a partial specific volume of 0.735 mL/g, which was calculated from the amino acid sequence.

Sigma or Boehringer-Mannheim.

Optical absorption was recorded at 25 °C on either a Shimadzu UV-260 or a Hitachi 100/80 recording spectrophotometer.

RESULTS

Sedimentation Equilibrium and Velocity of MnSOD. *E. coli* MnSOD (0.25 mg/mL, 100 μL) was dialyzed for 96 h at 4 °C against several 2-L changes of KPi , at 50 mM with 0.1 mM EDTA at pH 7.8 or at 200 mM without EDTA at pH 7.0. The enzyme in these two solvents was brought to sedimentation equilibrium at 18 000 rpm. Graphs of $\ln A_{280\text{nm}}$ against the square of the distance from the center of rotation fit straight lines over the entire cell length as shown in Figures 1 and 2. The partial specific volume of MnSOD was calculated to be 0.735 mL/g according to the method described by Schachman (1957) based upon the amino acid composition derived from the full sequence reported by Takeda and Avila (1986) and Steinman (1978). The slopes of the lines in Figures

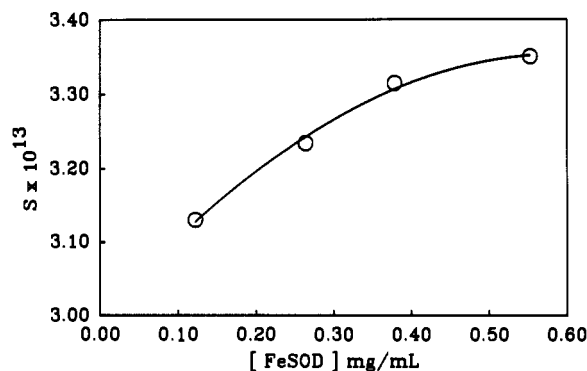


FIGURE 3: Sedimentation velocity of purified FeSOD. A total of 300 μ L of the enzyme in 50 mM KPi –0.1 mM EDTA (pH 7.8) was analyzed at the indicated protein concentrations. Rotor speed was 44 000 rpm, $\eta = 0.9888$ cP, and $T = 19^\circ\text{C}$. The movement of the boundary was monitored at 280 nm.

1 and 2, along with the density of the solvent, the temperature, and the calculated molecular weight, are given in Table I. The values of $45\,825 \pm 500$ obtained in the 50 mM buffer and $43\,027 \pm 250$ in the 200 mM buffer are in good agreement with the molecular weight of 45 800 calculated for the dimer from the amino acid sequence.

We have previously reported (Keele et al., 1970) a molecular weight for the *E. coli* MnSOD of 39 500. This was based upon an assumed partial specific volume of 0.720, rather than the calculated value of 0.735, and the data were collected with interference optics. In the previous study, as at present, there was no evidence of nonlinearity in the data when graphed according to Yphantis (1964). It follows that the enzyme behaves as a dimer with no discernible tendency toward either dissociation or aggregation, under these conditions.

The sedimentation velocity of MnSOD in 50 mM potassium phosphate + 0.1 mM EDTA, pH 7.8 and at 20°C , was examined with protein concentrations in the range 0.10–1.0 mg/mL. The results ranged from 3.7 S at 0.1 mg/mL to 3.2 S at 1.0 mg/mL. The s value extrapolated to zero protein concentration was 3.55 ± 0.3 S. The data obtained by sedimentation velocity and equilibrium allow calculation of a Stokes radius $R_s = 29 \pm 1.7$ Å. This may be compared with $R_s = 23.8$ Å calculated for an unhydrated sphere of molecular weight = 45 800 and partial specific volume of 0.735 mL/g. The frictional ratio for MnSOD (f/f_{\min}) is calculated to be 1.22, which is in the range characteristic of globular proteins.

Sedimentation Velocity and Equilibrium of FeSOD. Sedimentation velocity ordinarily increases as protein concentration decreased, as was the case with MnSOD, because retarding protein–protein interactions become less of a problem as the concentration is reduced. The sedimentation velocity of FeSOD was anomalous in that it decreased with diminishing protein concentration, as shown in Figure 3. This behavior is diagnostic of dissociation (Tanford, 1961; Van Holde, 1975), which was likely to have been rapid compared to the time scale of these sedimentation velocity measurements since there was no evidence for a second boundary of monomer at a rotor speed of 44 000 rpm.

Sedimentation equilibrium at 18 000 rpm gave evidence of two species, as shown in Figure 4. The molecular weight toward the top of the fluid column, where the protein concentration was low, was approximately 21 000, while at the bottom, where the protein concentration was high, it was approximately 37 000. This is the behavior expected from a monomer \rightleftharpoons dimer equilibrium.

FeSOD at 150 μ g/mL in 50 mM potassium phosphate–0.1 mM EDTA, pH 7.8, was equilibrated at 18 000, 22 000, and

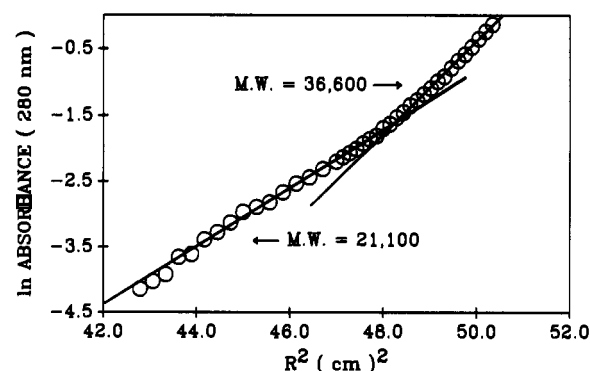


FIGURE 4: Sedimentation equilibrium of dialyzed FeSOD in 50 mM KPi (pH 7.8) buffer containing 0.1 mM EDTA. The protein (300 μ L) was brought to equilibrium at 18 000 rpm.

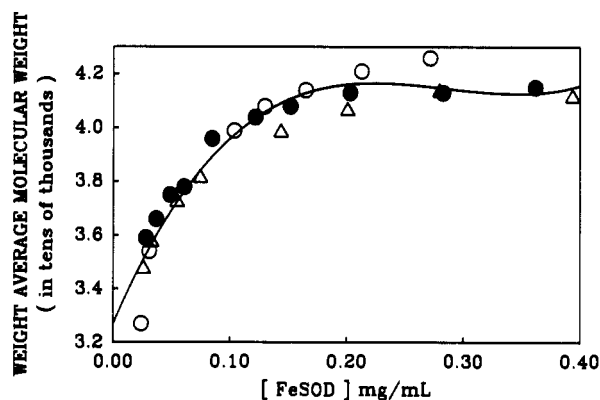


FIGURE 5: Sedimentation equilibrium of dialyzed native FeSOD at different rotor speeds. The enzyme was in 50 mM KPi –0.1 mM EDTA, pH 7.8. Data from the $\ln A_{280\text{nm}}$ vs R^2 plot at each rotor speed were fit to a third-order polynomial. The slope of the line at various positions from the center of rotation was calculated from the equation for the polynomial fit and converted to average molecular weight, which is plotted here as a function of protein concentration. $\nu = 0.733$ mL/g, $\rho = 1.006$ g/mL, and $T = 18^\circ\text{C}$. (○) 18 000, (●) 22 000, and (Δ) 26 000 rpm.

26 000 rpm. The data at all three rotor speeds yielded curved lines when $\ln A_{280\text{nm}}$ was graphed against R^2 . These data were fit to a third-order polynomial, according to a linear regression method. The weight-average molecular weight (M_{wr}) was calculated at several positions in the fluid column and thus at several different protein concentrations with the expression

$$\frac{d(\ln c)}{dr^2} = \frac{\omega^2(1 - \bar{v}\rho)}{2RT} M_{wr}$$

where $d(\ln c)/dr^2$ = slope of tangent to the curved line generated by graphing $\ln A_{280\text{nm}}$ versus R^2 , ω^2 = angular velocity in rad/s , \bar{v} = partial specific volume in mL/g, ρ = density of the solvent in g/mL, R = gas constant (8.314×10^7 erg $\text{mol}^{-1} \text{K}^{-1}$), and T = temperature in K.

The results of these manipulations of the sedimentation equilibrium data are shown in Figure 5. The molecular weight of FeSOD approached a limit of 42 000 at high protein concentration (0.4 mg/mL) and decreased sharply at concentrations lower than 0.15 mg/mL. These are again the properties expected for a dimer \rightleftharpoons monomer equilibrium. The possible influence of nonideality due to electrostatic effects was explored by repeating these studies in 0.2 M potassium phosphate at pH 7.0. The results at the higher ionic strength and lower pH were not noticeably different than those shown in Figure 5. Pressure gradients from the top to the bottom of the column of fluid, due to the centrifugal field, are another possible source of error. Pressure effects can likely be discounted, in the present case, because the data from three

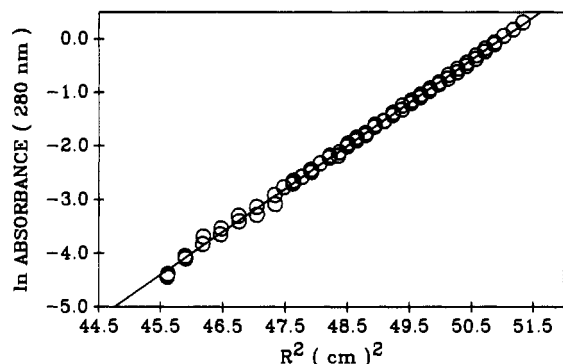


FIGURE 6: Sedimentation equilibrium of *undialyzed*, purified FeSOD at 18 000 rpm. The protein (5.4 mg/mL) was diluted to 0.15 mg/mL in 50 mM KPi (pH 7.8) buffer containing 0.1 mM EDTA.

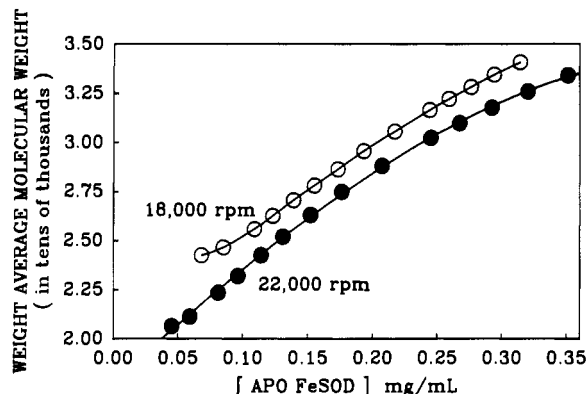


FIGURE 7: Sedimentation equilibrium of apoFeSOD in 50 mM KPi (pH 7.8) buffer–0.25 mM DTT containing 0.1 mM EDTA at 18 000 and 22 000 rpm. Data from the $\ln A_{280\text{nm}}$ vs R^2 plot at each rotor speed were fit to a third-order polynomial. The slope of the line at various positions from the center of rotation was calculated from the equation for the polynomial fit and converted to average molecular weight, which is plotted here as a function of protein concentration. (O) 18 000 and (●) 22 000 rpm.

different rotor speeds, and therefore three different pressure gradients, fall approximately on the same line, as shown in Figure 5 (Schachman, 1959; Howlett et al., 1970).

Effects of Dialysis. Both MnSOD and FeSOD had been equilibrated with the buffer by extensive dialysis prior to placement in the centrifugal field. It appeared possible that the very different equilibrium behavior of these two proteins might have been a consequence of dialysis. This was explored even though the activities of these enzymes were not significantly affected ($\pm 10\%$) by dialysis.

A stock solution of FeSOD at 5.4 mg/mL was diluted to 0.15 mg/mL with 50 mM KPi + 0.1 mM EDTA, pH 7.8, and was loaded directly into the ultracentrifuge cell and brought to equilibrium at 18 000 rpm. The data in Figure 6 indicate homogeneity, from the top to the bottom of the cell, and allow calculation of a unique molecular weight of 42 600. When the sample was examined at 44 000 rpm, a single sedimenting boundary was seen whose rate of sedimentation was $s = 3.22$ S. These data allowed calculation of the Stokes radius $R_s = 28.4$ Å.

Since dialyzed FeSOD gave evidence of dissociation, whereas the undialyzed enzyme did not, it appeared possible that dissociation was a property of the apoenzyme produced by metal loss during dialysis. ApoFeSOD at 100 $\mu\text{g/mL}$ in 50 mM KPi , 0.1 mM EDTA, and 0.25 mM DTT, at pH 7.8, was brought to equilibrium at 18 000 and at 22 000 rpm. Weight-average molecular weights were calculated at different positions in the fluid column, and therefore at different protein concentrations, and the results are presented in Figure 7. At

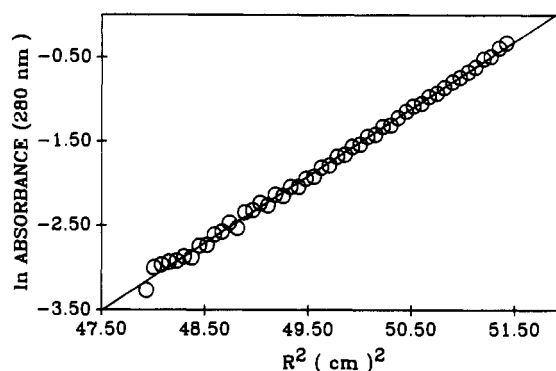


FIGURE 8: Sedimentation equilibrium of iron-reconstituted apoFeSOD. The enzyme was brought to equilibrium in 50 mM KPi –0.25 mM DTT (pH 7.8) at 18 000 rpm.

Table II: Summary of Analytical Ultracentrifuge Data for FeSOD and MnSOD

	MnSOD	FeSOD
$s^{20} (\times 10^{-13} \text{ s})^a$	3.55 ± 0.3	3.22 ± 0.3
$R_s (\text{Å})^b$	29.0 ± 1.7	28.5 ± 1.3
$R_{\text{min}} (\text{Å})^{b,c}$	23.8	23.1
f/f_{min}	1.22	1.23
mol wt ^a	$45\,800 \pm 500$	$42\,600 \pm 600$
$\bar{v} (\text{mL/g})^d$	0.735	0.733

^a Determined in 50 mM potassium phosphate (pH 7.8) buffer containing 100 μM EDTA. ^b Stokes radius. ^c Calculated by assuming an unhydrated sphere of $M = 45\,800$ for MnSOD or $42\,200$ for FeSOD. ^d Partial specific volume calculated from the amino acid sequence.

the low end of the concentration range studied (~ 0.1 mg/mL), the apoFeSOD is predominantly monomeric and at higher concentrations exists as a mixture of monomer and dimer, and possibly of small amounts of higher multimers. On the basis of the previous data, we estimate that at 150 $\mu\text{g/mL}$ undialyzed FeSOD is fully dimeric, dialyzed FeSOD is 19 mol % monomeric, and apoFeSOD is ~ 90 mol % monomeric.

When apoFeSOD was reconstituted with iron, as previously described (Beyer & Fridovich, 1987), we achieved 65% recovery of the starting material and a specific activity slightly lower (4700 units/mg) than that of the initial native enzyme (5000 units/mg). This reconstituted FeSOD, when brought to sedimentation equilibrium at 18 000 rpm, appeared homogeneous, from the top to the bottom of the fluid column, as shown in Figure 8. The molecular weight calculated for the reconstituted FeSOD is $42\,000 \pm 200$. Table II summarizes the data obtained with dialyzed MnSOD and with reconstituted FeSOD. Both of these enzymes are dimeric globular proteins whose molecular weights obtained from ultracentrifugation agree very well with those calculated from their amino acid sequences.

Sedimentation Equilibrium Properties of ApoMnSOD. We have seen that FeSOD lost metal during dialysis, whereas MnSOD did not, and that the differences in sedimentation equilibrium properties between these two dialyzed enzymes were due to dissociation of apoFeSOD. One must then inquire whether MnSOD would also dissociate when bereft of its metal. MnSOD at 0.25 mg/mL in 50 mM KPi + 0.1 mM EDTA, pH 7.8, was dialyzed for 16 h at 4 °C against 250 volumes of 2.5 M guanidinium chloride, 5 mM Tris, and 20 mM 8-hydroxyquinoline at pH 3.5. It was then dialyzed against several changes of cold 50 mM Tris + 0.1 mM EDTA at pH 7.8, followed by several changes of cold 50 mM KPi + 0.1 mM EDTA at pH 7.8. This procedure, which was devised for reversible resolution of MnSOD (Ose & Fridovich, 1976), yielded apoMnSOD that retained less than 0.2% of the activity of the holoenzyme.

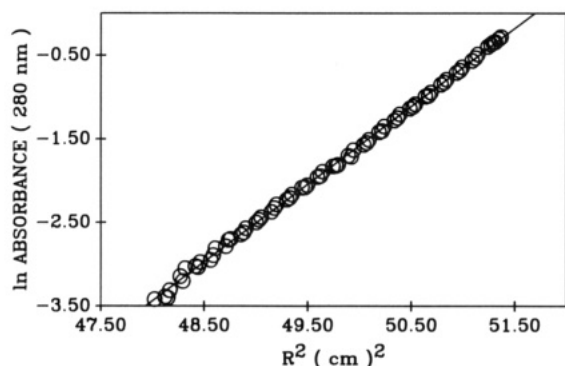


FIGURE 9: Sedimentation equilibrium of apoMnSOD at 18 000 rpm in 50 mM KPi (pH 7.8) buffer containing 0.1 mM EDTA. The apoenzyme had a specific activity of $\sim 0.2\%$ of that of the holoenzyme. A total of 91% of the initial optical density at 280 nm was recovered.

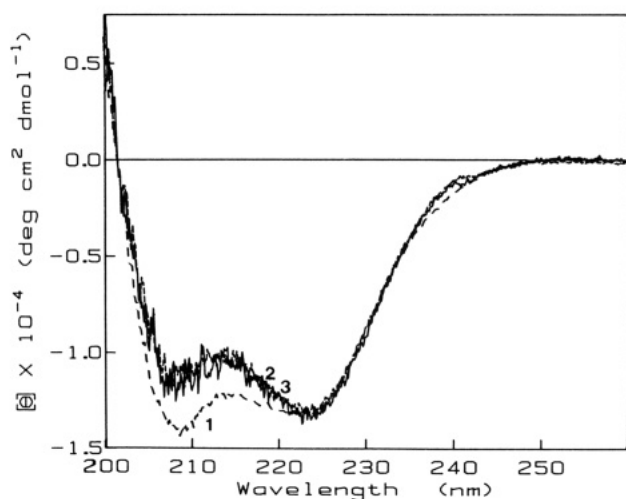


FIGURE 10: Circular dichroism of FeSOD. The UV circular dichroism spectra of undialyzed native FeSOD, dialyzed native FeSOD, and apoFeSOD were recorded in 50 mM KPi (pH 7.8) buffer containing 0.1 mM EDTA. A mean residue weight of 109.95 was used for the calculation of molar ellipticity ($[\theta]$). Protein concentrations were $\sim 100 \mu\text{g/mL}$, and the data presented here are an average of three scans: (line 1, ---) apoFeSOD; (line 2, —) undialyzed native FeSOD; (line 3, ...) dialyzed native FeSOD).

This apoMnSOD was brought to sedimentation equilibrium at 18 000 rpm. The Dintzis plot of the distribution of the apoenzyme in the ultracentrifugal cell is shown in Figure 9. The slope of this line, with the calculated $\bar{v} = 0.735 \text{ mL/g}$ and the density of the buffer = 1.006 g/mL , allowed calculation of a molecular weight of $48\,700 \pm 300$. The linearity of the data in Figure 9 indicates that apoMnSOD, unlike apoFeSOD, exhibits no tendency to dissociate. The apoMnSOD used in obtaining the data in Figure 9 was then reconstituted with Mn(II) , with recovery of 70% of the initial enzymatic activity.

Circular Dichroism. The equilibrium data indicated that holoFeSOD exists primarily as a homodimer, while the apoenzyme readily dissociates. Extensive dialysis appeared to cause some metal loss and therefore some dissociation into the monomeric form. It appeared likely that metal loss would be associated with some conformational effect detectable with CD. Figure 10 shows that dialysis of FeSOD did not cause significant changes in its CD spectrum but that removal of the iron increased the magnitude of the 207-nm band while not affecting the 222-nm band or the wavelength at which zero ellipticity (θ) occurs. These results indicate that metal removal is consistent with some increase in random structure. The mean residue ellipticity at 222 nm was $-1.33 \times 10^4 \text{ deg cm}^2 \text{ dmol}^{-1}$ for all three samples. This was based upon a mean

Table III: Fluorescence Parameters for Purified FeSOD and MnSOD^a

sample	mg/mL	emission, λ_{max} (nm)	Trp (μM)	rel intensity
native FeSOD ^b				
dialyzed	0.08	338	26.5	38.2
undialyzed	0.08	338	26.5	39.5
apoFeSOD ^b	0.08	342	26.5	72.6
native MnSOD ^c	0.07	345	19.3	27.5
apoMnSOD ^c	0.07	345	19.3	46.7
tryptophan ^d		355	11.4	41.5

^a Samples were present in 50 mM potassium phosphate buffer (pH 7.8) with 0.1 mM EDTA. Excitation was at 280 nm. ^b A molecular weight of 42 200 and 14 Trp per dimer were used to calculate the Trp concentration (μM). ^c A molecular weight of 45 800 and 12 Trp per dimer were used to calculate the Trp concentration (μM). ^d Concentration was determined by measuring the absorption at 278 nm and by using $\epsilon_{278} = 5700 \text{ M}^{-1} \text{ cm}^{-1}$.

residue weight of 109.95, which was calculated from the sequence data (Carlioz et al., 1988). The α -helical content was estimated from the mean residue ellipticity at 222 nm to be 36.3% (Chen & Yang, 1971).

Fluorescence. Because the fluorescence of tryptophan is very sensitive to its microenvironment, conformational changes can often be detected fluorometrically. When excited at 280 nm, FeSOD emitted a broad band centered at 338 nm with a quantum efficiency per tryptophan of 0.42 relative to that of free tryptophan in the same buffer. Dialysis of FeSOD caused only a very slight increase in this quantum efficiency, but removal of iron shifted the emission maximum to 342 nm and almost doubled the quantum efficiency. MnSOD differed markedly from FeSOD in its fluorescence behavior. Thus, MnSOD emitted maximally at 345 nm and with a lower quantum efficiency than FeSOD. Table III summarizes these fluorescence data. The effect of metal removal on the fluorescence of FeSOD has been noted previously for the enzyme from *P. ovalis* (Yamakura, 1978) and is not surprising given the positioning of tryptophan and tyrosine residues around the metal binding sites of both MnSOD and FeSOD (Stallings et al., 1983, 1985).

DISCUSSION

The MnSOD and FeSOD of *E. coli* are homodimeric globular proteins whose molecular weights derived from sedimentation equilibrium agree very well with those calculated from their amino acid sequences. These enzymes exhibit substantial differences when examined in solution. Thus, the apoenzyme derived from MnSOD can be reconstituted and reactivated with manganese but not with iron (Ose & Fridovich, 1976), while the activity of apoFeSOD can be reconstituted with iron but not with manganese. Our findings now indicate that removal of the metal from FeSOD diminishes the interaction between subunits and allows substantial dissociation. In contrast, MnSOD shows no detectable dissociation whether in the holo or in apo state. In both cases reconstitution with the appropriate metal cation resulted in restoration of the native activity, indicating that the apoenzymes being studied had not suffered significant irreversible denaturation. Indeed, circular dichroism indicated that both holo- and apoFeSODs contained $\sim 36\%$ α -helix.

The fluorescence quantum efficiency of FeSOD, on a per tryptophan basis, is nearly twice that of MnSOD. In both cases removal of the prosthetic metal nearly doubles the quantum efficiency, which is consistent with the clustering of tryptophan residues close to the metal binding sites (Stallings et al., 1984, 1985; Parker & Blake, 1988a,b). The position of the tryptophan emission maximum is in agreement with the

hydrophobic environment indicated from the X-ray structures. The MnSOD emission is about 7 nm shifted to the red, suggesting that the *average* tryptophan environment in *E. coli* MnSOD and FeSOD may be slightly different. In the *E. coli* enzymes, all of the tryptophans are in conserved regions except for one additional residue present in the iron enzyme (Carlioz et al., 1988).

These differences in solution properties between the MnSOD and FeSOD of *E. coli* would lead one to suggest potential structural differences, yet MnSODs and FeSODs are proposed to be structural homologues (Stallings et al., 1984). It would seem reasonable on the basis of the studies presented here to expect some subtle differences between *E. coli* FeSOD and MnSOD, at the contact interface.

At the present time, high-resolution crystallographic data (2.4 Å) are available only for the dimeric MnSOD from *B. stearothersophilus* (Parker & Blake, 1988a) and the tetrameric MnSOD from *T. thermophilus* HB8 (Stallings et al., 1985). The crystal structures for the FeSODs from *P. ovalis* (Ringe et al., 1983) and *E. coli* (Stallings et al., 1983) have been determined to 2.9 and 3.1 Å, respectively. Recently, the nucleotide sequence of the *E. coli* FeSOD was reported, and a new molecular model based on the DNA sequence and the 3.1-Å X-ray data allowed a detailed comparison of the iron enzyme with the MnSOD from *T. thermophilus* (Carlioz et al., 1988). The structural similarities revealed by such a comparison proved to be more extensive than was indicated in earlier studies. This analysis showed that the active site regions of the two enzymes are remarkably similar and are surrounded by a network of conserved aromatic residues. Of particular interest to the present study are the observations that the monomer contacts are close to the active site metal and the integrity of the interface is strengthened through hydrogen-bonding interactions that involve one of the metal ligands (His-160 in FeSOD). FeSOD residues Glu-159 and Tyr-163 (equivalent residues 169 and 173 in *T. thermophilus* MnSOD) penetrate into the metal-ligand environment of the adjoining subunit and hydrogen bond with the symmetry-related Tyr-163 and Glu-159 in the adjoining subunit. The insertion of tyrosine into the adjoining subunit contributes to the hydrophobic environment of the active site. Additional interchain contacts near the active center involve Asx-149 and Phe-127. Stabilization of the *T. thermophilus* tetrameric structure is achieved in part via contacts arising from a small helix (residues 55–62) that is absent in the *P. ovalis* and *E. coli* FeSOD structures.

The subunit interface detected in the dimeric MnSOD from *B. stearothersophilus* is different from that observed for the tetrameric *T. thermophilus* MnSOD and the *E. coli* FeSOD. Thus, there is no main-chain penetration of residues across the dimer interface as is observed for the *E. coli* and *T. thermophilus* enzymes (Parker & Blake, 1988a). The dimeric structure is stabilized via two hydrophobic interactions involving Phe-126 and Trp-165 and seven hydrogen-bonding interactions involving His-30, Ser-128, Glu-166, His-167, and Tyr-170. It is significant to note that of the six MnSODs and three FeSODs that have been sequenced, alignment for maximum homology indicates the positions of these residues are invariant, suggesting that the contact interfaces in the different proteins are very similar (Parker & Blake, 1988b). In addition, the role of the metal ligand, His-167, in strengthening the dimeric structure is also observed.

It was noted previously that almost every residue that penetrates the metal-ligand environment is conserved in all of the known sequences of FeSODs and MnSODs. One ex-

ception is the substitution of Phe in MnSOD for Tyr at position 76 in FeSOD (Carlioz et al., 1988). A close examination of the active site presented for the *E. coli* FeSOD suggests a potential interaction between Tyr-76 and Tyr-173. The proximity of the residues is interesting considering the drastically different conditions that are required for the preparation of the apoenzymes of FeSOD and MnSOD. Thus, preparation of apoMnSOD requires a hydrophobic chelator such as 8-hydroxyquinoline and low pH (3.5) in the presence of either 8 M urea or 2.5 M Gdn-HCl. Conversely, preparation of apoFeSOD is only efficacious when high pH (9–11), EDTA, and the presence of an electron donor such as dithiothreitol are used. MnSOD is not resolved with the procedure for preparation of apoFeSOD, and no native apoFeSOD is recovered when the treatment used for resolution of MnSOD is applied. On the basis of the proximity of Tyr-76 and Tyr-173 in the *E. coli* FeSOD, we could envisage that, at the high pH required for metal removal, ionization of these tyrosine residues would result in electrostatic repulsion between the two phenolate moieties, perhaps facilitating iron removal by altering the cavity environment. An equivalent repulsion would not be observed in the MnSOD due to the replacement of this tyrosine with phenylalanine.

It has been noted that FeSOD sequences show relatively high identity (65–75%) among the different sources and tend to be more closely related to each other than to any prokaryotic MnSOD (Parker & Blake, 1988b). The *E. coli* FeSOD has a higher degree of sequence homology with the *B. stearothersophilus* MnSOD (49%) than either *T. thermophilus* MnSOD (40%) or *E. coli* MnSOD (42%). The crystallographic data clearly indicate that there are subtle differences in the monomer contact interfaces between the MnSODs from *B. stearothersophilus* and *T. thermophilus*. Variations in the sequence of *B. stearothersophilus* distinctly favors the formation of a dimeric structure over the tetrameric structure observed with *T. thermophilus*. Dissociation of the oligomeric MnSOD molecule has been suggested to account for both the release and the incorporation of manganese during reconstitution of *B. stearothersophilus* enzyme (Brock et al., 1976). Is it possible that in the *E. coli* enzymes local interactions are different in apoMnSOD and apoFeSOD such that dimer formation is more favored in one than in the other?

Not until the structure of the MnSOD from *E. coli* is known will it be possible to see to what extent it is homologous to the FeSOD from the same organism. Our results lead us to expect that subtle structural differences will be found.

Registry No. SOD, 9054-89-1.

REFERENCES

- Bannister, J. V., Bannister, W. H., & Rotilio, G. (1987) *CRC Critical Rev. Biochem.* 22, 111.
- Beyer, W. F., Jr., & Fridovich, I. (1986) in *Manganese in Metabolism and Enzyme Function* (Schramm, V. L., & Wedler, F. C., Eds.) p 193, Academic Press, New York.
- Beyer, W. F., Jr., & Fridovich, I. (1987) *Biochemistry* 26, 1251.
- Brock, C. J., Harris, J. I., & Sato, S. (1976) *J. Mol. Biol.* 107, 175.
- Carlioz, A., Ludwig, M. L., Stallings, W. C., Fee, J. A., Steinman, H. M., & Touati, D. (1988) *J. Biol. Chem.* 263, 1555.
- Chen, Y. H., & Yang, J. T. (1971) *Biochem. Biophys. Res. Commun.* 44, 1285.
- Davis, B. J. (1964) *Ann. N.Y. Acad. Sci.* 121, 404.
- Fridovich, I. (1986) *Adv. Enzymol. Relat. Areas Mol. Biol.* 58, 61.

- Howlett, G. J., Jeffrey, P. D., & Nichol, L. W. (1970) *J. Phys. Chem.* 74, 3607.
- Keele, B. B., Jr., McCord, J. M., & Fridovich, I. (1970) *J. Biol. Chem.* 245, 6176.
- Laemmli, V. R. (1970) *Nature (London)* 227, 680.
- Martin, M. E., Byers, B. R., Olson, M. D., Salin, M. L., Arceneaux, J. E. L., & Tolbert, C. (1986) *J. Biol. Chem.* 261, 9361.
- McCord, J. M., & Fridovich, I. (1969) *J. Biol. Chem.* 244, 6049.
- Meier, B., Barra, D., Bassa, F., Calabrese, L., & Rotilio, G. (1982) *J. Biol. Chem.* 257, 13977.
- Misra, H. P., & Fridovich, I. (1978) *Arch. Biochem. Biophys.* 189, 317.
- Murphy, J. B., & Kies, M. W. (1960) *Biochim. Biophys. Acta* 45, 382.
- Ose, D. E., & Fridovich, I. (1976) *J. Biol. Chem.* 251, 1217.
- Parker, M. W., & Blake, C. C. F. (1988a) *J. Mol. Biol.* 199, 649.
- Parker, M. W., & Blake, C. C. F. (1988b) *FEBS Lett.* 229, 377.
- Pennington, C. D., & Gregory, E. M. (1986) *J. Bacteriol.* 166, 528.
- Ringe, D., Petsko, G. A., Yamakura, F., Suzuki, K., & Ohmori, D. (1983) *Proc. Natl. Acad. Sci. U.S.A.* 80, 3879.
- Schachman, H. K. (1957) *Methods Enzymol.* 4, 65.
- Schachman, H. K. (1959) in *Ultracentrifugation in Biochemistry*, p 174, Academic Press, New York.
- Schinina, M. E., Maffey, L., Barra, D., Bossa, F., Puget, K., & Michelson, A. M. (1987) *FEBS Lett.* 221, 87.
- Stallings, W. C., Powers, T. B., Patridge, K. A., Fee, J. A., & Ludwig, M. C. (1983) *Proc. Natl. Acad. Sci. U.S.A.* 80, 3884.
- Stallings, W. C., Patridge, K. A., Strong, R. K., & Ludwig, M. L. (1984) *J. Biol. Chem.* 259, 10695.
- Stallings, W. C., Patridge, K. A., Strong, R. K., & Ludwig, M. L. (1985) *J. Biol. Chem.* 260, 16424.
- Steinman, H. M. (1978) *J. Biol. Chem.* 253, 8708.
- Takeda, Y., & Avila, H. (1986) *Nucleic Acids Res.* 14, 4577.
- Tanford, C. T. (1961) *Physical Chemistry of Macromolecules*, Wiley, New York.
- Van Holde, K. E. (1975) in *The Proteins* (Neurath, H., & Hill, R. L., Eds.) Vol. 1, p 225, Academic Press, New York.
- Yamakura, F. (1978) *J. Biochem.* 83, 849.
- Yamakura, F., & Suzuki, K. (1976) *Biochem. Biophys. Res. Commun.* 72, 1108.
- Yang, J. T., Wu, C. C., & Martinez, H. M. (1986) *Methods Enzymol.* 130, 208.
- Yphantis, D. A. (1964) *Biochemistry* 3, 297.

Volume Changes in the Binding of Lanthanides to Peptide Analogues of Loop II of Calmodulin[†]

Donald W. Kupke*[‡] and Jay W. Fox[§]

Departments of Biochemistry and Microbiology, School of Medicine, The University of Virginia, Charlottesville, Virginia 22908

Received August 15, 1988; Revised Manuscript Received February 3, 1989

ABSTRACT: The solution expansion accompanying coordination of lanthanide ions to synthetic peptide analogues of a metal-binding loop in calmodulin was determined by a density method. This study was designed to further test the hypothesis that the nonlinear expansions observed upon sequential addition of Ca²⁺ to intracellular calcium-binding proteins reflect principally upon the coordination event at specific binding sequences. Three peptides of 13 residues each were synthesized as analogues of binding loop II in mammalian calmodulin: Peptide I was the native analogue; peptide II contained an aspartyl in place of an asparaginyl residue at position 5 from the N-terminus; for peptide III, the aspartyl residue in position 3 of the native analogue was interchanged with the asparaginyl residue in position 5. Thus, the number of charged-oxygen donor atoms for coordination was the same in I and in III, but the latter peptide could permit two pairs of acidic groups to converge toward the metal ion as in some loops of these proteins. The observed expansions with different lanthanide ions to the same peptide varied appreciably, suggesting dissimilar structures [Gariépy et al. (1983) *Biochemistry* 22, 1765-1772]; coordination to the simpler tetracarboxylate sequestrants, on the other hand, generated an expansion profile approximately as expected from the properties of the lanthanide series. The largest expansions were generated with peptide II (having the additional acidic group) for all lanthanides tested. The smaller expansions seen with peptide III as compared to those for peptide I indicate that the free peptides do not adopt configurations like that comprising the apo-binding cavities in this class of proteins, wherein a putative overlap of electrostatic fields from converging carboxylate groups is frozen in. The distinctive volume changes attending these coordinations support the proposition that the volume property reflects small differences in coordinating sequences. Thus, volume change may be applied efficaciously to those proteins in which a sequential uptake of metal ion to multiple sites is manifested.

Considerable information on the intracellular calcium-binding proteins has been generated by studying metal-ion binding to

synthetic peptide analogues of selected sequences within these proteins. A particular aspect has dealt with spectral studies on the binding of various lanthanide ions to peptide analogues (12-13 residues) of the calcium-binding loops within these proteins (Reid et al., 1980; Marchiori et al., 1983; Kanellis et al., 1983; Gariépy et al., 1983, 1985; Pavone et al., 1984; Buchta et al., 1986; Malik et al., 1987). These peptides do

[†]This investigation was supported by a research grant (GM-34938) from the U.S. Public Health Service.

[‡]Department of Biochemistry.

[§]Department of Microbiology.